Materials for Energy
Workshop "Advances in Fuel Cells and Hydrogen"
April 2010, Torres Vedras, Portugal

INFLUENCE OF CATALYST SUPPORT CHARACTERISTICS AND FUNCTIONALIZATION ON THE CATALYTIC ACTIVITY OF Pt-Ru FOR PEM FUEL CELLS

J.C. CALDERÓN[(1)], J.L. FIGUEIREDO[(2)], N. MAHATA[(2)], M.F.R. PEREIRA[(2)], V.R. FERNANDES[(3)]
C.M. RANGEL[(3)], L. CALVILLO[(4)], M.J. LÁZARO[(4)], E. PASTOR[(1)*]

(1) Departament of Physical Chemistry, Institute of Materials and Nano-technology, University of La Laguna, Avda Astrofísico Francisco Sánchez s/n, 38071 – La Laguna, Tenerife (Spain)
(2) Catalysis and Materials Laboratory, LSRE/LCM, University of Porto, 4200-465 – Porto (Portugal)
(3) LNEG, Fuel Cells and Hydrogen Unit, Estrada do Paço do Lumiar 22, 1649-038 – Lisbon (Portugal)
(4) CSIC – Instituto de Carboquímica, Miguel Luesma Castán 4, 50018 – Zaragoza (Spain)
* epastor@ull.es

ABSTRACT: Pt-Ru electrocatalysts supported on carbon xerogels and ordered mesoporous carbons were synthesized by reduction with formate ions (SFM method). Chemical and heat treatments were applied to modified the surface chemistry of original carbon supports. Physical characterization of the catalysts was performed using X-ray dispersive energy (EDX) and X-ray diffraction (XRD) techniques, while the electrochemical activity towards methanol oxidation was studied by cyclic voltammetry (CV). Pt-Ru catalysts with nominal metal content (20 wt.%) and atomic ratios (Pt:Ru 1:1) were successfully synthesized on the different supports. Higher methanol oxidation current densities were obtained for those supports with a higher content of surface oxygen groups. Gas diffusion electrode and membrane-electrode-assembly preparation allowed an in-house built of a direct methanol fuel monocell for the evaluation of the catalysts performance. Polarization curves were measured confirming the results obtained in a three electrodes electrochemical cell by CV. Normalized power curves per weight of Pt are discussed in terms of the significant impact on noble metal loading and attained cell maximum power, in comparison with results obtained with a commercial catalyst.

Keywords: carbon xerogels, CMK-3 ordered mesoporous carbons, Pt-Ru electrocatalysts, polymer electrolyte membrane fuel cells.

RESUMO: Electrocalisadores de Pt-Ru suportados em xerogel de carbono e carbonos mesoporosos ordenados foram sintetizados por redução com iões formato. Foram implementados tratamentos térmicos e químicos para a modificação da química de superfície dos carbonos utilizados. A caracterização física dos catalisadores foi realizada utilizando as técnicas de difracção de Raio-X (DRX) e espectroscopia por energia dispersiva de Raios-X (EDX), enquanto a actividade electroquímica para a oxidação do metanol foi estudada por voltametria cíclica (VC). Catalisadores de Pt-Ru com semelhante teor de metal (20 wt.%) e raios atómicos (Pt:Ru 1:1) foram sintetizados com sucesso nos diferentes suportes. Foram obtidas maiores densidades de corrente na oxidação do metanol para os suportes com maior teor de grupos oxigénio na superfície. Eléctrodos de difusão gasosa e o conjunto eléctrodo-membrana foram preparados no laboratório para construção de uma célula de combustível de metanol directo, com vista ao estudo do desempenho dos catalisadores. Foram efectuadas curvas de polarização que confirmaram os resultados obtidos por VC numa célula electroquímica de três eléctrodos. Curvas de potência, normalizadas por peso de Platina, são discutidas em termos do impacto significativo da quantidade de metal nobre e potência máxima atingida pela célula, em comparação com os resultados obtidos com um catalisador comercial.

Palavras-chave: xerogel de carbono, carbono mesoporoso ordenado CMK-3, electrocatalisadores Pt-Ru, células de combustível de membrana de electrólito polimérico.

1. INTRODUCTION

Anodic catalysts for polymer electrolyte membrane fuel cells (PEMFC) are conformed by Pt-Ru nanoparticles supported on carbon black, usually Vulcan XC-72 [1], but recent works have shown that graphite nanofibers [2,3], carbon nanotubes [4-9], carbon microspheres [10,11], hard carbon spherules [12], carbon aerogels and xerogels [9,13,14] as well as mesoporous carbons [15,16] can improve the efficiencies of the catalysts, when they are used as supports. Causes for such efficiency enhancement are related to the metal dispersion increase, nanoparticle agglomerates decrease and electrochemical species diffusion and conductivity improvement. However, there are other important aspects related to the role of carbon support in catalyst performance. For example, some authors have reported the increase of electronic density on catalytic particles by a donor effect of the carbon support [17]. This effect is explained from the decrease of the Fermi level, which modifies the Galvani potential of the catalyst [18]. It is considered that oxygen groups on the carbon surface allow the specific metal-support interaction, promoting the electron transfer from platinum clusters to the carbon support [19]. Therefore, Pt-carbon support interaction is beneficial to the catalytic properties [20], improving nanoparticles stability [21]. Nevertheless, the rise in electron density can be significant only if double layer thickness is comparable to the metal microdeposit size. This double layer is formed between the nanoparticle and the carbon support [18]. One way for determining the electrocatalytic activity due to the synergism between carbon support and catalytic nanoparticles, considering the electronic state of Pt when this is deposited on the carbon support [22], is making use of the difference in the electronic work functions of platinum (5.4 eV) and the carbon support (4.7 eV), which results in an increase of the electron density on Pt. Dependence between particle size and double layer thickness has been described by means of a model who considers a tetrahedron hypothetical shape for the metal particle [23]. In these conditions, double layer and nanoparticle volumes keep the ratio of 0.6, 1.0, 1.5 and 2.0 in the edge size, for microdeposit amounts to 71, 42, 28, and 21%, making evident the influence of particle size on the metal-carbon interaction. Different methodologies have been used for studying these interaction effects, like electron-spin resonance (ESR) and X-ray photoelectron spectroscopy (XPS), showing the dependence between electron donation by Pt to the carbon support and Fermi-level [24,25].

Moreover, surface functional groups play a key role in the interaction between carbon support and metal precursor. H_2PtCl_6 and $[Pt(NH_3)_4]Cl_2$ are the typical precursors in Pt/C synthesis in acid and basic media, respectively. Interaction between H_2PtCl_6 and carbon is coordinated by a redox process, which involves an oxidation state change to Pt^{2+} [26]. Pt^{2+} links to oxygen groups, basic sites which act as good anchoring sites for the Pt^{4+} present in hexachloroplatinic anion. These sites have a Lewis structure and are associated with π-electron rich regions within the basal planes [27-29].

Carbon xerogels can be used as carbon supports, because of their structural properties, like high porosity, high surface area, controllable pore size, and different form (monolith, thin film, or powder) [30]. This material has been used in environmental applications [31,32], fuel cells [9,14,33,], and different types of reactions [34-36]. On the other hand, ordered mesoporous carbons have recently received great attention because of their potential use as catalytic supports in fuel cell electrodes. They have controllable pore sizes, high surface areas and large pore volumes [30]. Nanoporous carbons with 3D ordered pore structures have been shown to improve the mass transport of reactants and products during fuel cell operation [18].

Deposition of catalytic particles on carbon support is possible by means of different synthesis methods such as the reduction by sodium borohydride (BM) or formic acid (FAM). Especially, FAM method does not completely reduce the Ru precursor salt, because of the low dissociation constant of formic acid (1.8×10^{-5}) and the pH dependence of the reduction potential of Ru.

In this study, a modified FAM method was used for carry out the Pt-Ru nanoparticles synthesis on functionalized carbons, in which the pH of the reaction medium was increased to 12, to certify complete dissociation of acid formic into formate ions, species that act as reducing agent (formate ion method-SFM) [37]. Synthesized catalysts were analyzed by different techniques for establishing their physicochemical properties. Furthermore, electrooxidation of CO and methanol were analyzed using cyclic voltammetry (CV) and chronoamperometry (CA). Finally, prepared materials were tested in a direct methanol fuel monocell, in order to verify performance and cell power densities when these catalysts are use as anodes.

2. EXPERIMENTAL

2.1. Carbon support synthesis

Carbon materials prepared as support for Pt-Ru catalysts were carbon xerogel (CX) and ordered mesoporous carbons (CMK-3). Carbon xerogels were synthesized by polycondensation of resorcinol with formaldehyde [38]. Resorcinol (Aldrich, 99%) was added to deionised water until complete dissolution. Then, formaldehyde solution (Sigma, 37 wt.% in water, stabilized with 15 wt.% methanol) was mixed with previously dissolved resorcinol. Concentrated sodium hydroxide solution was added under continuous stirring in order to obtain the desired initial pH of the precursor solution (6.0). pH was monitored because of this parameter plays a key role in the mesoporous formation of carbon xerogels [38]. Gelation was performed at 358 K during 72 hours. Then, gel was shaped to 0.1 mm particles and dried defining a heating ramp from 333 to 423 K during 5 days, with a 20 K day^{-1} rate increase. Finally, gel was pyrolyzed at 1073 K under nitrogen flow, obtaining a carbon xerogel, hereafter referred as CXUA. Carbon materials were treated with 7 M HNO_3 in a soxhlet for 3 h, washed and dried at 110°C (sample CXNA). Additional samples were prepared by heat treatment at different tem-

peratures: 30 min at 400 (CXNA400), 600 (CXNA600) and 750ºC (CXNA750). CMK-3 materials were obtained by incipient wetness impregnation method using ordered mesoporous silica as template and a furan resin as carbon precursor [39]. The impregnated silica was carbonized at 700°C for 2 h and subsequently, the silica-carbon composite was subjected to washing with NaOH in ethanol to remove the silica. Then, these carbons were functionalized by treatment with either diluted or concentrated nitric acid for 0.5 h (CMK-3 NdTa05 and CMK-3 NcTa05, respectively).

2.2. Carbon xerogel characterization

Textural characterization of carbon materials was made by means of N_2 adsorption isotherms, obtained at 77 K with a Quantachrome NOVA 4200e multi-station apparatus. BET analysis of isotherms was used to determine specific surface area (S_{BET}), micropore volumes (V_{MIC}) and non-microporous surface areas (mainly mesopores, S_{MES}) [40].

2.3. Ordered mesoporous carbon characterization

BET analysis was made using a Micromeritics ASAP 2020. Before carrying out the analysis, the samples were degassed to reach a stable vacuum of 10^{-5} mmHg.

2.4. Pt-Ru catalysts synthesis

Formate ions reduction method (SFM method) was used to synthesize Pt-Ru catalysts with a nominal metal loading of 20 wt.% and an atomic ratio Pt:Ru of 1:1. Carbon materials were dispersed in a 2.0 M HCOOH solution with pH previously adjusted to 12.0. Then, the mixture was heated at 80ºC, and a 1.13 mM solution of both Pt and Ru metal salt precursors (H_2PtCl_6, 8% p/p solution, Aldrich; and $RuCl_3$, 99.999%, Aldrich) was added under stirring. Temperature was kept constant during slowly addition of metal precursors. Reaction medium was kept under stirring for 12 h, and finally, the mixture was filtered, washed and dried at 60ºC for 2 h.

2.5. Physical characterization

Metal content and Pt-Ru atomic ratios of the synthesized catalysts were determined by means of energy dispersive X-ray (EDX), using analysis by a scanning electron microscope (LEO Mod. 440) at 20 keV, with a Si detector and a Be window. X-ray diffraction (XRD) patterns were obtained using a universal diffractometer Panalytical X´Pert operating with Cu-Kα radiation generated at 40 kV and 30 mA. Scans were done at 3º min^{-1} for 2θ values between 20 y 100º. Scherrer's equation was used to calculate the metal crystallite size using the (220) peak around 2θ = 70°, and the lattice parameter was evaluated from the peaks values for (111), (200), (220) and (311) crystalline faces by refining the unit cell dimensions by the least squares method .

2.6 Electrochemical characterization

An electrochemical cell with three electrodes was used for the electrochemical characterization of the synthesized catalysts. A glassy carbon bar and a reversible hydrogen electrode (RHE) placed inside a Luggin capillary were used as counter and reference electrodes, respectively. All measured potentials in the text are referred to the RHE. For preparing the working electrode, a catalyst ink was obtained using 2 mg of catalyst, 15 μL of Nafion® (5 wt.%, Aldrich) and 500 μL of ultra-pure water, and deposited on a glassy carbon disk. 0.5 M H_2SO_4 (95-97%, Merck) was used as supporting electrolyte. Potentiostatic measurements were carried out employing a μ-AUTOLAB III modular equipment. High resistivity deoxygenated 18.2 MΩ H_2O was used for the preparation of all the electrolyte and methanol solutions. The electrocatalytic activity of prepared materials was compared to that of the commercial PtRu (1:1, 20 wt.%)/C catalyst from E-TEK. Electroactive areas were calculated from CO adsorption, in order to express obtained current densities in respect to the active electrochemical area.

2.7. Direct methanol fuel monocell tests

Electrodes used for membrane electrode assemblies (MEAs) consist of a diffusion layer and a catalyst layer. The gas diffusion layers were prepared from carbon black Vulcan XC-72 R for the anodes and the cathodes. Pt-Ru catalysts were used as anodes and 10 wt.% Pt/C catalyst was used as cathode. To fabricate the catalyst layer, an ink was prepared by suspending the material in isopropanol, and stirring in an ultrasonic bath for 10 min to thoroughly wet and disperse it. A 5% Nafion® dispersion solution (Electrochem, Inc) was then added to the mixture. The catalyst inks were dispersed onto the gas diffusion layer with a brush, and dried at 50°C, until a catalyst loading of 4 mg cm^{-2} was achieved. Nafion® 117 membranes were cleaned and converted into the acid form by boiling in 3% H_2O_2 for 1 h, followed by boiling in 0.5 M H_2SO_4 for 2 h. Between these treatments, the membranes were washed with boiling water for 30 minutes. The cleaned membranes were stored in ultrapure water. Each MEA was assembled by hot-pressing the prepared anode and cathode on either side of the pretreated membrane at 50 bar and 130°C for 180 s. MEAs were placed into an in-house built direct methanol fuel monocell hardware. A monocell configuration was used with 25 cm^2 of active area and a single serpentine flow field design drawn on graphite plates. A test station allowed conditioning of the cell and reactants at temperatures up to 70ºC for activation and polarisation curve recording. Monocells were operated with a 0.75 M aqueous CH_3OH solution pumped through the anode compartment at 1.5 mL min^{-1}. O_2 was fed through the cathode compartment at 0.3 L min^{-1}. After the preconditioning procedure of the MEA previously described [41], polarization curves were measured.

3. RESULTS AND DISCUSSION

3.1. Carbon support characterization

Textural properties of carbon supports were determined by N_2 physisorption, BET analysis, whereas the surface chemistry was analyzed by TPD experiments (data not shown).

Carbon xerogel showed a mesoporous morphology (average pore diameter size = 16.5 nm) with surface areas in the range 632-754 m^2g^{-1}. Surface chemistry was found to depend on the chemical and heat treatment used. In contrast, CMK-3 materials presented an ordered structure, maintained even after the oxidation treatments, with carbon nanorods of uniform size arranged in the same direction, leaving mesopores between them. They showed high surface areas (769-1163 m^2g^{-1}) and large pore volumes (0.51-0.81 cm^3g^{-1}). Pore size distribution was close to 3 nm. The number of surface oxygen groups increased with the HNO_3 treatments, but both the specific surface area and pore volume decreased slightly.

3.2. Physicochemical characterization of synthesized Pt-Ru catalysts

XRD patterns were obtained for the synthesized catalysts. All of them presented the characteristic peaks of the face centred cubic (fcc) structure of Pt, (111), (200), (220) and (311), with values in degrees near to those observed for the E-TEK commercial catalyst. For all prepared materials, metal loadings and atomic ratios were closed to nominal values (20 wt.% and Pt:Ru 1:1). Similar crystallite sizes were calculated from XRD for PtRu/CX, in the range 4.1 ± 0.5 nm, which are also analogous to the 4.4 nm obtained for the E-TEK catalyst. An influence of the support is observed when ordered mesoporous carbon was used: PtRu nanoparticles prepared on CMK-3 displayed smaller sizes, especially after chemical treatment with a decrease from 3.8 to 2.9 nm. Lattice parameters were lower than the 3.92 Å corresponding to Pt, indicating the formation of an alloy between Ru and Pt.

3.3. Methanol electrooxidation

Cyclic voltammetry for the electrochemical oxidation of methanol at room temperature for the electrocatalysts supported on carbon xerogels and CMK-3 carbon can be seen in Fig. 1a and Fig. 1b, respectively. In the case of catalysts supported on carbon xerogels, PtRu/CXNA was showed the highest methanol oxidation current density. However, all synthesized catalysts displayed higher current densities than that obtained for commercial PtRu/C E-TEK. It is noticeable that methanol oxidation current densities decreased as the heat treatment temperature of carbon xerogels increased. For catalysts supported on ordered mesoporous carbons, it was found that the strength of the chemical treatment benefited the methanol electrochemical oxidation (Fig. 1b).

From these results it can be deduced that the presence of oxygenated groups plays an essential function in the electrochemical behaviour of synthesized catalysts. In the case of carbon xerogels, the best electrochemical behaviour was obtained for catalysts without heating treatment of the carbon support. The loss of oxygenated groups occurs with increasing the temperature of the heat treatment: carboxylic acid groups and lactones decompose into CO_2 at 400ºC and 600ºC, respectively, whereas anhydrides produce CO and CO_2 at 750ºC. At the last temperature, only oxygenated species which are not removed are phenol, carbonyl, ether and quinone groups [42].

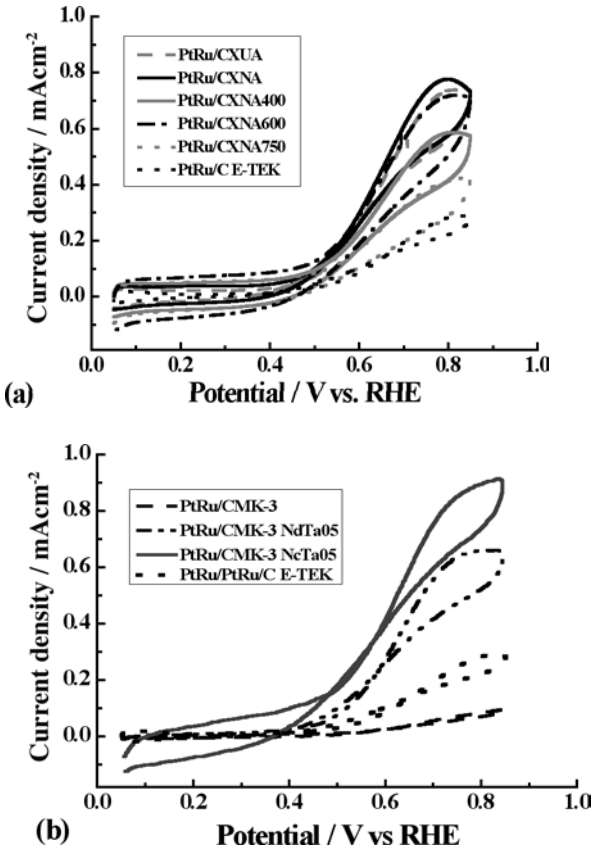

Fig. 1. Cyclic voltammograms for methanol electrochemical oxidation on synthesized PtRu catalysts, supported on (a) carbon xerogels and (b) ordered mesoporous carbons.
Scan rate: 20 mVs^{-1}. Supporting electrolyte: 0.5 M H_2SO_4. Methanol concentration: 2.0 M.

In the case of the CMK-3 materials, the total amount of oxygenated groups is increased with the severity of the chemical treatment [15]. Thus, the catalyst prepared with the original material (CMK-3) displayed a very low activity, but increasing the number of surface oxygen groups resulted in a drastic increase in the response of the materials towards the methanol electrooxidation.

According to these results, surface oxygenated groups are important in the electronic transfer process between the catalytic nanoparticle and the carbon support and consequently, the presence of these groups on the carbon surface promotes the methanol electrochemical oxidation.

3.4 Direct metanol fuel monocell tests

3.4.1. Polarization curves

In order to determine synthesized PtRu catalysts efficiencies, direct methanol fuel monocell tests were performed. Figure 2 shows the polarization curves obtained for those catalysts supported on carbon xerogels which presented the highest (PtRu/CXNA) and lowest (PtRu/CXNA750) current densities in Fig. 1a.

It was observed that the potential drop diminished with increasing the operational temperature of the monocell. On the other hand, comparing both materials, PtRu/CXNA (Fig. 2a) displayed lower potential drops and higher current densities,

in agreement with the electrochemical characterization results in Fig. 1a. Thus, monocell tests confirm the decrease in performance as the temperature of the heat treatment of the carbon xerogel increases.

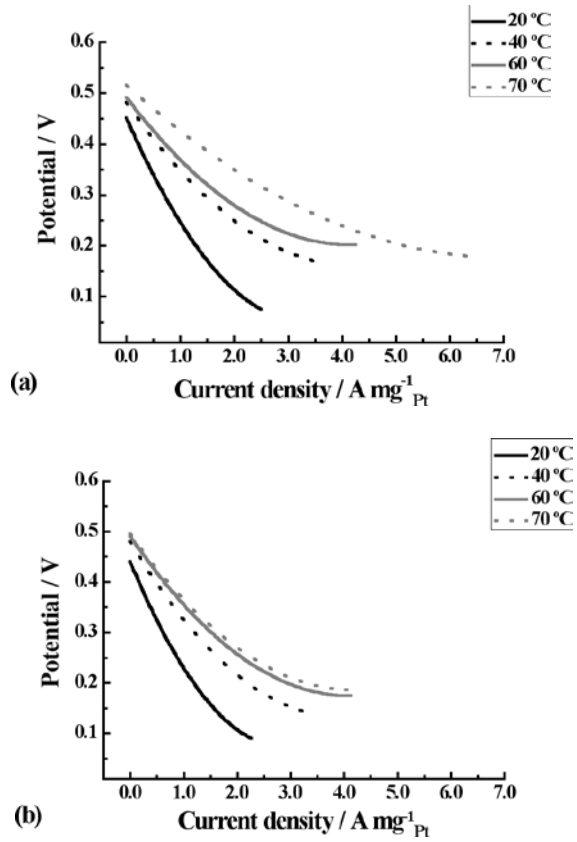

Fig. 2. Polarization curves for a DMFC monocell at different temperatures, using Pt-Ru catalysts supported on carbon xerogels as anodes: (a) PtRu/CXNA and (b) PtRu/CXNA750. Cathode: 10 wt.% Pt/C. Concentration and methanol solution flux: 0.75 M and 15 mL min^{-1}, respectively. Oxygen flux: 0.3 L min^{-1}.

Comparison between polarization curves for PtRu catalysts supported on the different carbon xerogels and the commercial PtRu/C E-TEK at 70ºC can be seen in Fig. 3. It can be observed that PtRu/CXNA displayed a similar response to that of the commercial catalyst, which shows the lowest potential drop.

In agreement with previous results in Figure 1a and Figure 2, from Figure 3 it can be concluded that the heating treatment

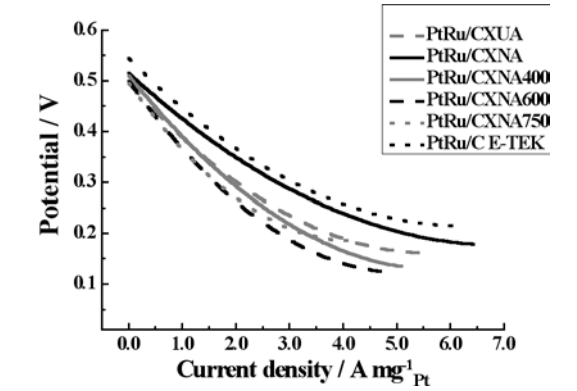

Fig. 3. Polarization curves for a DMFC monocell at 70ºC, using Pt-Ru catalysts supported on carbon xerogels as anodes. Cathode: 10 wt.% Pt/C. Concentration and methanol solution flux: 0.75 M and 15 mL min^{-1}, respectively. Oxygen flux: 0.3 L min^{-1}.

of the carbon support does not promote the enhancement of the monocell performance.

Also for Pt-Ru catalysts supported on CMK-3 ordered mesoporous carbons, polarization curves were obtained (Fig. 4). For these catalysts, current densities were much lower than those obtained for Pt-Ru catalysts supported on carbon xerogels.

These results were unexpected, taking into account the results showed in Fig. 1, and could be related to the electrical conductivity of the catalysts layer, which determines the behaviour in the monocell configuration.

In concrete, this property depends strongly on the electrical conductivity of the material used as catalyst support. In this case, CMK-3 carbon has a very low electrical conductivity (~ 10^{-2} S cm^{-1}) that results in a high ohmic resistance during the electrochemical measurements and consequently, a poor fuel cell performance. However, it is possible to observed differences for the three CMK-3 based catalysts. PtRu nanoparticles supported on CMK-3 NdTa05 and CMK-3 NcTa05 (Fig. 4b and c, respectively) displayed higher current densities than the catalyst supported on CMK-3 (Fig. 4a), but similar between them. Again, the importance of the oxygenated groups on carbon surface was highlighted.

Accordingly, the commercial catalyst PtRu/C E-TEK showed better performance than the PtRu catalysts supported on CMK-3 ordered mesoporous carbons (Fig. 5).

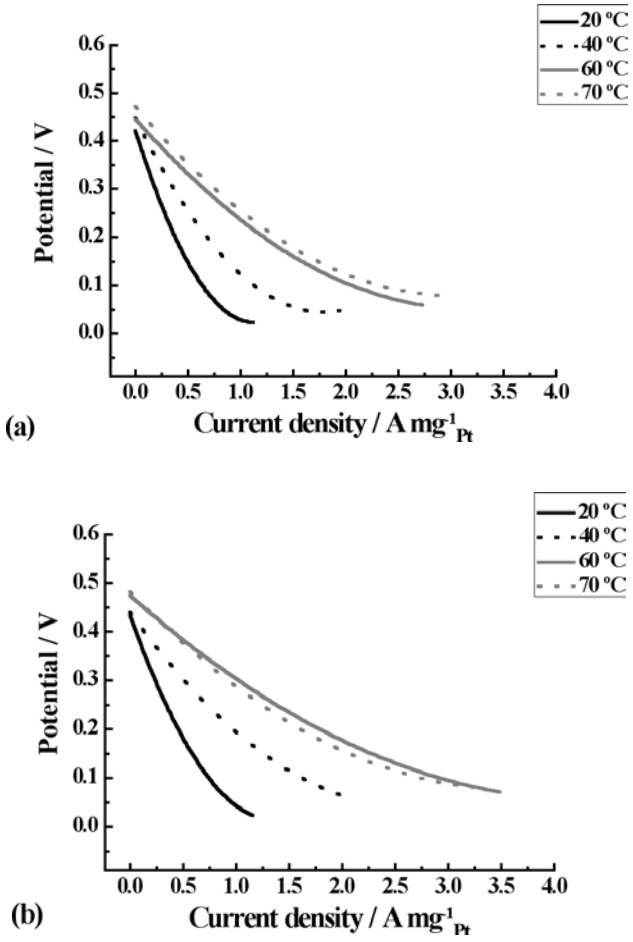

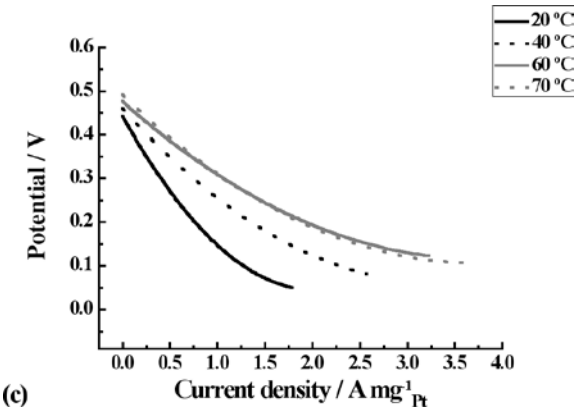

Fig. 4. Polarization curves recorded in a DMFC monocell at different temperatures using Pt-Ru catalysts supported on CMK-3 ordered mesoporous carbons as anodes: (a) PtRu/CMK-3, (b) PtRu/CMK-3 NdTa05, (c) PtRu/CMK-3 NcTa05. Cathode: 10 wt.% Pt/C. Concentration and methanol disolution flux: 0.75 M and 15 mL min^{-1}, respectively. Oxygen Flux: 0.3 L min^{-1}.

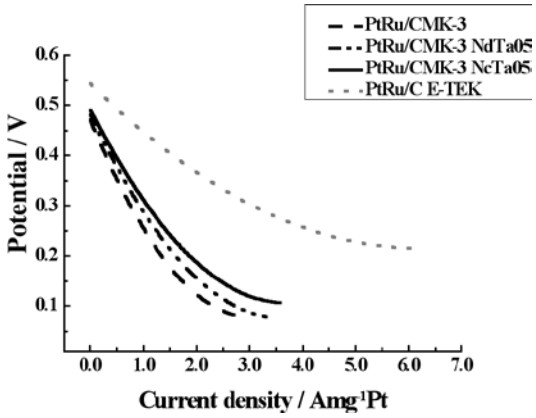

Fig. 5. Polarization curves for a DMFC monocell at 70ºC using Pt-Ru catalysts supported on CMK-3 ordered mesoporous carbons as anodes. Cathode: 10 wt.% Pt/C. Concentration and methanol solution flux: 0.75 M and 15 mL min^{-1}, respectively. Oxygen Flux: 0.3 L min^{-1}.

3.4.2 Power density curves

Figs. 6 and 7 show the power density curves (normalized by Pt content) for the catalysts supported con carbon xerogels and CMK-3 carbons, respectively. Curves were obtained from data in Figs. 3 and 5. It can be observed that catalysts supported on carbon xerogels subjected to heat treatments presented the lowest performance in DMFC (Fig. 6). However, the good performance registered for PtRu/CXNA was confirmed.

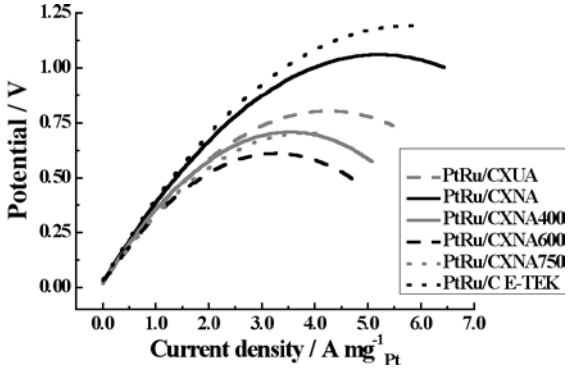

Fig. 6. Power density curves for a DMFC monocell at 70ºC using Pt-Ru catalysts supported on carbon xerogels as anodes. Cathode: 10 wt.% Pt/C. Concentration and methanol solution flux: 0.75 M y 15 mL min^{-1}, respectively. Oxygen flux: 0.3 L min^{-1}.

In the case of catalysts supported on CMK-3 ordered mesoporous carbons (Fig. 7), following the previous results, power densities were lower than those obtained for PtRu catalysts supported on carbon xerogels (Fig. 6) and chemical treatments produced a clear increase in the performance of the catalyst, but in all cases lower power densities than that for PtRu/C E-TEK were recorded.

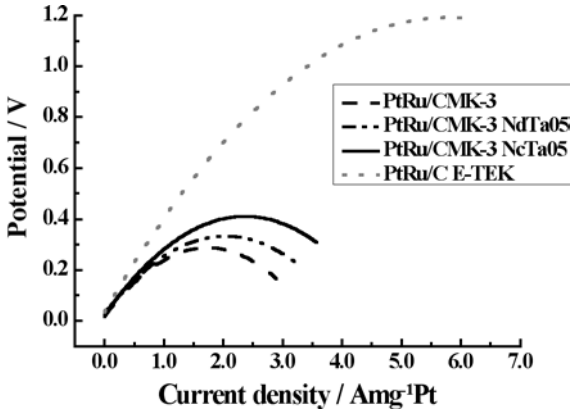

Fig. 7. Power density curves for a DMFC monocell at 70ºC using Pt-Ru catalysts supported on CMK-3 ordered mesoporous carbons as anodes. Cathode: 10 wt.% Pt/C. Concentration and methanol solution flux: 0.75 M and 15 mL min^{-1}, respectively.Oxygen flux:0.3 L min^{-1}.

4. CONCLUSIONS

PtRu catalyst supported on carbons xerogels and CMK-3 ordered mesoporous carbons were prepared with metal loading and Pt:Ru proportions closed to 20 wt.% and 1:1, respectively. Crystallite sizes were about 4.1 ± 0.5 nm, for catalysts supported on carbon xerogels, whereas they were around 2.9 nm for catalysts supported on CMK-3 carbons.

Lattice parameters were lower than 3.92 Å, indicating the formation of an alloy between platinum and ruthenium.

Electrochemical characterization for catalysts supported on carbon xerogels confirmed the great influence of the heating treatment of the carbon supports on the catalytic properties.

For the methanol electrochemical oxidation, a decrease of the current densities was observed as the temperature of the treatment increased. For catalysts supported on CMK-3 ordered mesoporous carbons, the strength of the chemical treatment promoted the oxidation of the alcohol. Catalysts supported on carbon xerogels exhibited good results as anode in a direct methanol fuel monocell, in terms of both potential drop and power density. Consequently, it was possible to correlate the electrocatalytic behaviour with the presence of some surface oxygenated groups on the carbon supports.

Finally, from this work PtRu/CXNA is proposed as good candidate for the anode of direct methanol fuel cells.

ACKNOWLEDGEMENTS

This work was carried out within the Acción Integrada Hispano-Portuguesa (E-25/09 and HP2008-036); J.C.C. is indebt-

ed to the Alβan Program for the predoctoral fellowship No. E07D403742CO, and NM to FCT for the postdoctoral grant BPD/14804/2003. Authors acknowledge the Spanish MICINN for financial support (MAT2008-06631-C03-01 and -02).

REFERENCES

[1] E. Antolini, Applied. Catalysis. B: Enviroment, 88 (2009) 1-24.

[2] C.A. Bessel, K. Laubernds, N.M. Rodriguez, R.T.K. Baker, Journal of Physical Chemistry B, 105 (2001) 1115-1118.

[3] E.S. Steigerwalt, G.A. Deluga, D.E. Cliffel, C.M. A Lukehart, Journal of Physical Chemistry B, 105 (2001) 8097-8101.

[4] W. Li, C. Liang, J. Qiu, W. Zhou, H. Han, Z. Wei, G. Sun, Q. Xin, Carbon, 40 (2002) 791-794.

[5] W. Li, C. Liang, W. Zhou, J. Qiu, H. Li, G. Sun, Q. Xin, Carbon, 42 (2003) 436 – 439.

[6] W. Li, C. Liang, W. Zhou, J. Qiu, Z. Zhou, G. Sun, Q. Xin, Journal of Physical Chemistry B, 107 (2003) 6292-6299.

[7] W. Chen, J.Y. Lee, Z. Liu, Materials Letters, 58 (2004) 3166-3169.

[8] H. Tang, J. H. Chen, Z.P. Huang, D.Z. Wang, Z.F. Ren, L.H. Nie, Y.F. Kuang, S.Z. Yao, Carbon 42 (2004) 191-197.

[9] J.L. Figueiredo, M.F.R. Pereira, P. Serp, P. Kalck, P.V. Samant, J. B. Fernandes, Carbon 44 (2006) 2516-2522.

[10] Y.C. Liu, X.P. Qiu, Y.Q. Huang, W.T. Zhu, Carbon, 40 (2002) 2375-2380.

[11] Y.C. Liu, X.P. Qiu, Y.Q. Huang, W.T. Zhu, Journal of Power Sources, 111 (2002) 160-164.

[12] R. Yang, X. Qiu, H. Zhang, J. Li, W. Zhu, Z. Wang, X. Huang, L. Chen, Carbon, 43 (2005) 11-16.

[13] J. Marie, S. Berthon-Fabry, P. Achard, M. Chatenet, A. Pradourat, E. Chainet, Journal of Non-Crystallyne Solids, 350 (2004) 88-96.

[14] N. Job, J. Marie, S. Lambert, S. Berthon-Fabry, P. Achard, Energy Conversion and Management, 49 (2008) 2461-2470.

[15] L. Calvillo, M.J. Lázaro, E.G. Bordejé, R. Moliner, P.L. Cabot, I. Esparbé, E. Pastor, J.J. Quintana, Journal of Power Sources, 169 (2007) 59-64.

[16] J. Ding, K-Y. Chan, J. Ren, F-S. Xiao, Electrochimica Acta, 50 (2005) 3131-3141.

[17] P. Gallezot, D. Richard, G. Bergeret, ACS Symposium Series, 437 (1990) 150-159.

[18] X. Yu, S. Ye, Journal of Power Sources, 172 (2007) 133-144.

[19] J. Escard, C. Leclère, J. P. Contour, Journal of Catalysis, 29 (1973) 31-39.

[20] J. C. Vedrine, M. Dufaux, C. Naccache, B. Imelik, Journal of Chemical Society, Faraday Transactions, 74, (1978) 440-449.

[21] A. Biloul, F. Coowar, O. Contamin, G. Scarbeck, M. Savy, D. van den Ham, J. Riga, J.J. Verbist, Journal of Electroanalytical Chemistry and Interfacial Electrochemistry, 289 (1990) 189-201.

[22] V.S.Bagotzky, A.M. Skundin, Electrochimica Acta, 29 (1984) 757-765.

[23] A. V. Kobelev, R. M. Kobeleva, V. F. Ukhov, Physica status solidi, 96 (1979) 169-176.

[24] L. J. Hillenbrand, J. W. Lacksonen, Journal of Electrochemical Society, 112 (1965) 249-252.

[25] F.Coloma, A. Sepúlveda-Escribano, J. L. G. Fierro, F. Rodríguez-Reinoso, Applied Catalysis A: General, 148 (1996) 63-80.

[26] S. R. de Miguel, O. A. Scelza, M. C. Román-Martínez, C. Salinas-Martínez de Lecea, D. Cazorla-Amorós, A. Linares-Solano, Applied Catalysis A: General, 170 (1998) 93-103.

[27] M.V. Lopez-Ramon, F. Stoeckli, C. Moreno-Castilla, F. Carrasco-Marin, Carbon, 37 (1999) 1215-1221.

[28] S.S. Barton, M. J. B. Evans, E. Halliop, J. A. F. MacDonald, Carbon, 35 (1997) 1361-1366.

[29] C.A. Leon, J.M. Solar, V. Calemma, L.R. Radovic, Carbon, 30 (1992) 797-811.

[30] N. Mahata, M.F.R. Pereira, F. Suárez-García, A. Martínez-Alonso, J.M.D. Tascón, J.L. Figueiredo, Journal of Colloid Interface Science, 324 (2008) 150-155.

[31] A.C. Apolinário, A.M.T. Silva, B.F. Machado, H.T. Gomes, P.P. Araújo, J.L. Figueiredo, Applied Catalysis B: Enviroment, 84 (2008) 75 – 86.

[32] H.T. Gomes, B.F. Machado, A. Ribeiro, I. Moreira, M. Rosário, A.M.T. Silva, Journal of Hazard Materials, 159 (2008) 420-426.

[33] C. Arbizzani, S. Beninati, E. Manferrari, F. Soavi, M. Mastragostino, Journal of Power Sources, 172 (2007) 578-586.

[34] S.A. Al-Muhtaseb, Carbon, 46 (2008) 1003-1009.

[35] N. Mahata, F. Gonçalves, M.F.R. Pereira, J.L. Figueiredo, Applied Catalysis A: General, 339 (2008)159-68.

[36] N. Job, B. Heinrichs, F. Ferauche, F. Noville, J. Marien, J.P. Pirard, Catalysis Today, 102–103 (2005) 234-241.

[37] L. dos Santos, F. Colmati, E. R. Gonzalez, Journal of Power Sources, 159 (2006) 869-877.

[38] N. Job, R. Pirard, J. Marien, J.P. Pirard, Carbon, 42 (2004) 619-628.

[39] M.J. Lázaro, L. Calvillo, E.G: Bordejé, R. Moliner, R. Juan, C.R. Ruiz, Microporous and Mesoporous Materials, 103 (2007) 158-165.

[40] F. Rodriguez-Reinoso, J.M. Martin-Martinez, C. Prado-Burguete, B. McEnaney, Journal of Physical Chemistry, 91 (1987) 515-516.

[41] A. Kulikovsky, H. Schmitz, K. Wippermann, J. Mergel, B. Fricke, T. Sanders, D.U. Sauer, Journal of Power Sources, 173 (2007) 420-423.

[42] A. Silva, B. Machado, J. L. Figueiredo, J. L. Faria, Carbon, 47 (2009) 1679-1679.